Map Description based on Angular Radon Spectrum

Ernesto Fontana[1] and Dario Lodi Rizzini[12]

***Abstract*— In this paper, we present a novel descriptor of point cloud maps based on Angular Radon Spectrum (ARS). ARS effectively characterizes the collinearity of 2D point sets and satisfies the properties of translation-invariance and shift-rotation. This descriptor can be used for globally optimal registration of point clouds as well as for mapping tasks including loop closure detection. Experiments have assessed high accuracy and robustness of ARS-based pose estimation.**

I. Introduction

Robot mapping is a critical problem for the execution of multiple tasks in mobile robotics. Range sensors like LIDARs and depth cameras are able to acquire geometrically accurate representations of the environment in the form of point clouds. The capability to estimate relative pose and similarity between two point clouds is required to compose a larger map. The problem of estimating the relative pose between point clouds acquired from different viewpoints is usually referred to as registration. Recognition of places already visited by the robot enables detection of loops in robot path and resolves potential inconsistencies. Both operations are generally the backbone for constructing stable and semantically strong maps. Robust features related to global geometric properties can effectively support consistent map building with measurements that, although accurate, lack in semantic characterization.

Literature on localization and mapping with range data is predominantly oriented to the occupancy grid map paradigm [1] that solves laser scan alignment and loop closure detection (LCD) through correlative registration. Alternative approaches are based on vector representation [2]. Landmark maps consist of keypoint features with descriptors extracted from laser scans. In this context, LCD is solved either through geometric relation signatures [3] or through bag-of-words (BoW) approach [4]. In the context of pose graph systems, outlier data association in LCD and registration can be found according to graph self-consistency [5], which has proven insufficient without explicit map representation. The survey by Yin *et al.* [6] considers many SLAM pipelines, categorizing them while posing special focus on the loop closure detection (or place recognition) method used. Angular Radon Spectrum (ARS) [7], [8] is a descriptor computed on point clouds represented in the form of Gaussian Mixture Model (GMM). It is based on Radon transform and represents in a continuous form the collinearity of a point set with respect to the direction of a pencil of parallel lines. ARS is suitable for registration and comparison between point clouds due to its invariance to translation and to the shift caused by rotation. The similarity between the spectra of two point clouds can be computed even without knowing their relative pose (e.g., without robot odometry).

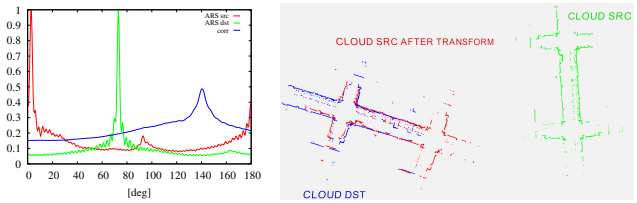

Fig. 1: Application of ARS to registration: on the left, subfigure a), spectra of ARS on source (red), destination (green) clouds and correlation (blue) between the two; on the right, subfigure b), shows the result of consecutive maps alignment through Anisotropic ARS.

In this paper we propose two applications of ARS for 2D mapping. The first application is planar point cloud registration: the estimation of rotation angle between two point clouds corresponds to the maximum of correlation between their spectra. Subsequently, the simplified problem of translation estimation alone can be addressed through global optimization techniques like consensus or branch-and-bound. The second application is candidate selection for place recognition in map building tasks. While ARS, as well as other geometric descriptors is not enough for disambiguation of places, it enables selection of candidate map patches for loop closure. Then, computationally expensive comparisons can be concentrated on the most promising candidates.

II. Angular Radon Spectrum

ARS is a descriptor defined for point clouds as Gaussian Mixture Models (GMM) [7], [8]. Each input point is associated to a Gaussian kernel centered on the point and a covariance matrix representing its uncertainty. Alternatively, the GMM can be inferred from the point concentration. Let $\mathcal{P} = \{\boldsymbol{\mu}_i\}_{i=1,\dots,n_p}$ with $\boldsymbol{\mu}_i \in \mathbb{R}^2$ be the estimated position vectors of the points. It is convenient to define the *density function* $f : \mathbb{R}^2 \to \mathbb{R}_{\geqslant 0}$ that represents the point density in the plane. Then, the said GMM density function is defined as

$$f(\boldsymbol{r}) = \sum_{i=1}^{n_p} w_i \; f_i(\mathbf{r}) = \sum_{i=1}^{n_p} w_i \; \mathrm{n}\left(\mathbf{r} - \boldsymbol{\mu}_i, \boldsymbol{\Sigma}_i\right) \qquad (1)$$

[1]Ernesto Fontana and Dario Lodi Rizzini are with RIMLab (Robotics and Intelligent Machines Laboratory), Dipartimento di Ingegneria e Architettura, University of Parma. 43124, Parco Area delle Scienze 181/A, Parma, Italy

[2]Dario Lodi Rizzini is also with Centro Interdipartimentale per l'Energia e l'Ambiente (CIDEA), University of Parma, 43124, Italy.

Emails: {ernesto.fontana, dario.lodirizzini}@unipr.it

where the sum of positive weights w_i is equal to 1 and symbol $\mathrm{n}\,()$ is used for a Gaussian kernel of mean value $\boldsymbol{\mu}_i$ and covariance matrix $\boldsymbol{\Sigma}_i$. The *Radon Transform* (RT) [9] of $f(\boldsymbol{r})$ enables to measure the alignment of the point set with a given line $\mathcal{F}_{\mathbf{q}}$ represented by parameters $\mathbf{q} = [\theta, \rho]^\top$. The RT is defined as

$$\mathcal{R}[f](\mathbf{q}) = \int_{\mathcal{F}_{\mathbf{q}}} f(\mathbf{r}) d\mathbf{r} = \sum_{i=1}^{n_p} w_i \int_{\mathcal{F}_{\mathbf{q}}} \mathrm{n}\,(\mathbf{r} - \boldsymbol{\mu}_i, \boldsymbol{\Sigma}_i)\, d\mathbf{r}. \quad (2)$$

In our case, the integral of the line $\mathcal{F}_{\mathbf{q}}$ can be solved through the parametric equation of the points $\mathbf{r}(\mathbf{t})$ lying on the line $\mathbf{r}(\mathbf{t}) = t_1\ \mathbf{u}_1 + t_2\ \mathbf{u}_2$, where $t_1 = \rho$ is fixed, t_2 is the varying parameter associated to the points on the line, $\mathbf{u}_1 = \hat{\mathbf{u}}(\theta) = [\cos\theta, \sin\theta]^\top$ is the unitary vector orthogonal to the line and $\mathbf{u}_2 = \hat{\mathbf{u}}(\theta + \pi/2) = [-\sin\theta, \cos\theta]^\top$ corresponds to the line direction. After the variable change from $\mathbf{r}$ to $\mathbf{t}$, eq. (2) is equivalent to the marginal of Gaussian distribution

$$\mathcal{R}[f_i](\theta, \rho) = \mathrm{n}\left(\rho - \tilde{\mu}_{i,1}, \tilde{\sigma}^2_{i,1}\right) \quad (3)$$

where $\tilde{\mu}_{i,1} = \mathbf{u}_1^\top \boldsymbol{\mu}_i$ and $\tilde{\sigma}^2_{i,1} = \mathbf{u}_1^\top \boldsymbol{\Sigma}_i \mathbf{u}_1$.

The ARS is a function applied to RT to detect patterns of points collinear to a given direction measured by θ. Given a superadditive concentration function $\kappa(x)$, the ARS is defined as

$$\mathcal{S}\,[f]\,(\theta) = \int_{-\infty}^{+\infty} \kappa\left(\mathcal{R}[f](\theta, \rho)\right)\ d\rho\ . \quad (4)$$

A standard concentration function is $\kappa(x) = x^2$, which is implicitly used in the remaining. Thus, the square of a sum of Gaussian kernels $\kappa(\mathcal{R}[f])$ in eq. (1) consists of double products of Gaussians that can be integrated. The equation of the ARS of a GMM has the form

$$\mathcal{S}\,[f]\,(\theta) = \sum_{i=1}^{n_p} \sum_{j=1}^{n_p} w_i\ w_j\ \psi_{ij}(\theta)\ . \quad (5)$$

The ARS kernel functions $\psi_{ij}(\theta)$ are equal to the Gaussian-like function

$$\psi_{ij}(\theta) = \mathrm{n}\left(\mathbf{u}_1^\top(\theta)(\boldsymbol{\mu}_i - \boldsymbol{\mu}_j), \mathbf{u}_1^\top(\theta)(\boldsymbol{\Sigma}_i + \boldsymbol{\Sigma}_j)\mathbf{u}_1(\theta)\right) \quad (6)$$

The equation of $\psi_{ij}(\theta)$ is simpler in the isotropic case, where each point belonging to input point cloud has a 1-on-1 corresponding Gaussian in the GMM, with center at the estimated point coordinates. The isotropic term comes from the fact that all Gaussians that compose the GMM have the same variance σ. The ARS $\mathcal{S}\,[f]\,(\theta)$ is π-periodic and can be expanded into a Fourier series. This expansion is exploited for the estimation of rotation. For a more in-depth look to the more intricate anisotropic case, please refer to [8].

The main property of ARS lies in its invariance to translation $\mathbf{t}$ and angular-shift. If a translation $\mathbf{t}$ and a rotation $\mathbf{R}$ with angle δ are applied to a point set represented by density function $f(\mathbf{r})$, then the spectrum of the transformed point set satisfy the equation

$$\mathcal{S}\,[f(\mathbf{R}(\delta)\ \mathbf{r} + \mathbf{t})]\,(\theta) = \mathcal{S}\,[f(\mathbf{r})]\,(\theta + \delta) \quad (7)$$

The property just expressed in eq. (7) is important for the estimation of rotation, as explained in the following.

ARS can be effectively used to compare point clouds for evaluation of the rigid transformation between them and for recognition of visited place. Let $f_S f(\mathbf{r})$ and $f_T f(\mathbf{r})$ be the density functions of source and, respectively, destination point clouds. Let $\mathcal{S}\,[f_S]$ and $\mathcal{S}\,[f_T]$ be the Angular Radon spectra corresponding to the respective point clouds. If $f_S f(\mathbf{r})$ and $f_T f(\mathbf{r})$ represent the same scenes from different viewpoints, than $\mathcal{S}\,[f_S]$ is the shifted copy of the $\mathcal{S}\,[f_T]$. The correlation function comparing the source spectrum rotated by angle δ and the destination spectrum is defined as

$$C[f_S, f_T](\delta) = \frac{1}{\pi} \int_0^{\pi} \mathcal{S}\,[f_S]\,(\theta + \delta)\ \mathcal{S}\,[f_T]\,(\theta)\ d\theta \quad (8)$$

Since each ARS can be represented as Fourier series, the correlation function is elegantly expressed in form of convolution. The correlation can be used to compute the rotation angle δ^* between two spectra representing the same scene, by searching the value δ^* that maximizes $C[f_S, f_T](\delta)$. With $C[f_S, f_T](\delta)$ in Fourier series form, the global maximum δ^* can be efficiently found through a branch-and-bound algorithm [7]. We observe that, since ARS is π-periodic, the real rotation angle is either δ or $\delta + \pi$. Next section illustrates how to disambiguate between the two values of rotation angle and to solve full global registration. Finally, the correlation function can be normalized and used to measures the similarity between ARS descriptors. Similarity is defined as

$$S[f_S, f_T] = \frac{\max_\delta C[f_S, f_S](\delta)}{C[f_S, f_S](0)\ C[f_T, f_T](0)}\ . \quad (9)$$

with values between 0 and 1. Next section presents how ARS comparison can be applied to robot mapping.

III. Mapping with ARS

ARS descriptor provides a representation of environment that is invariant to viewpoint changes and, hence, is suitable for comparison of submaps. This section presents two applications: registration of submaps and selection of candidates for loop closure.

Through ARS, rotation estimation can be formulated as maximization of correlation according to equations (8) and (9). The global maximum of correlation can be efficiently found using a branch-and-bound procedure. Due to the π periodicity of ARS, the rotation angle is either δ^* or $\delta^* + \pi$. The assessment of translation enables disambiguation between the two candidate values of rotation. We have investigated several algorithms for translation, once the two candidate rotation angles are available. To complete global registration, we choose a branch-and-bound procedure inspired by [10]. The objective function to be maximized is the number of overlapping point pairs between destination and the translated source point clouds. A point pair is overlapping if their distance is less than tolerance ϵ. Given a closed box $\mathcal{B} \subset \mathbb{R}^2$, the lower and upper bounds of the number of matching pairs are estimated.

Another application that has been considered is loop closure detection based on ARS similarity. Given a point cloud $\mathcal{C}$ representing the current submap or laser scan, the goal is to search other submaps $\mathcal{L}_i$ potentially representing the same map portion. The submaps $\mathcal{C}$ and $\mathcal{L}_i$ can be geometrically matched (e.g., counting the associated point pairs), after the two point clouds are properly aligned. However, registration of $\mathcal{C}$ with a large set of candidate loops $\mathcal{L}_i$ is computationally infeasible. A solution is to compare their ARS $\mathcal{S}[f_{\mathcal{C}}]$ and $\mathcal{S}[f_{\mathcal{L}_i}]$ in order to select the most promising candidate matches. The similarity in eq. (9) can be computed efficiently. The proposed approach is to find the k submaps with larger values of $S[f_{\mathcal{C}}, f_{\mathcal{L}_i}]$. Thus, full geometric matching is reserved on these candidates.

IV. Experiments

The first set of experiments has been conducted on standard benchmarks of planar laser scans for robot localization and mapping applications: *fr079*, *fr-clinic*, *intel-lab* and *mit-csail*. Each of said datasets contains about 5000 scans. The goal of the conducted experiments is to correctly estimate the rigid transformation between subsequent scans in each dataset. Pose estimation tests have been separated into rotation and translation estimation respectively. For rotation, we compared results obtained with six methods through the ground truth information contained in the datasets, as explained in [8]. Translation has been estimated after rotating the point clouds by an angle estimated through Isotropic ARS. Results are reported in Figure 2. ARS methods achieve an error on-par or lower than the other rotation estimation methods, while just a bit over the 1 cm scan resolution parameter when estimating translations. It has to be noted that several failed estimations are due to non-overlapping scans.

The second group of tests is designed to assess ARS-based registration on 2D occupancy grid maps. The dataset chosen for this test, called hereafter *unipr-dia*, has been acquired using a Pioneer 3DX, equipped with a Sick LMS100 and a multi-layer LIDAR Velodyne VLP16, in the main hallways of the Dipartimento di Ingegneria e Architettura at the University of Parma. Two separate sequences called *uniprdia_0* and *uniprdia_1* have been used. The raw laser scans and odometry measurements from these datasets have been processed by mapping tool Cartographer [1], whose map has been used as ground truth. The proposed ARS registration algorithm has been compared with Hector SLAM (briefly, Hector) [11] and Cartographer [1]. At each iteration, the estimation given by ARS is based only on the alignment of current laser scan with the previous one, without initial guess. Conversely, Hector and Cartographer are full mapping systems that align and merge each new scan with the current map. Moreover, Hector uses the initial guess provided by the robot odometry, while Cartographer also integrates the 3D measurements from the LIDAR. The goal of such comparison is to display the robustness of ARS estimation, albeit based on scan-to-scan comparison. Figure 4 displays the occupancy grid maps (only sequence *uniprdia_1* is shown due to limited space), as well as the estimated trajectories obtained with the three methods. The occupancy grid maps are obtained through online collection and merging of the aligned laser scans using Octomap [12], for a fair comparison of the three approaches. Even though it uses less data, ARS is able to estimate locally accurate trajectories. Table I reports the Average Translational Error (ATE) and Average Rotational Error (ARE) for Hector and ARS with respect to the trajectory of Cartographer (used as ground truth) in the two sequences. As expected, ARS errors are larger, but significantly limited for a scan matching algorithm.

TABLE I: Average Translational Error (ATE) and Average Rotational Error (ARE) obtained by Hector and ARS on the given sequences of datasets *uniprdia_0* and *uniprdia_1*.

Dataset	Length [m]	Hector		ARS	
		ATE [%]	ARE $[10^{-2\circ}/m]$	ATE [%]	ARE $[10^{-2\circ}/m]$
uniprdia_0	262.28	3.87	7.18	19.78	31.66
uniprdia_1	180.34	3.14	6.66	11.06	32.58

Finally, a third set of experiments assesses the capability of ARS correlation to select loop closure candidates on the already mentioned laser scan datasets. Figure 3 compares ARS correlation and the distance between two submaps from datasets *fr079*, *fr-clinic*, *intel-lab* and *mit-csail*. ARS correlation only slightly decreases with the distance between the reference frames of two submaps, thus weakly discriminating between true and false matching regions of the maps.

V. Conclusion

This paper has presented follow-up work on the ARS registration pipeline. Capability of ARS descriptor in place recognition task, and improvements of the translation estimation algorithm have been discussed. The branch-and-bound based translation estimation method presented has improved precision and accuracy significantly. Loop closure detection based on ARS correlation only discriminates potentially matching map regions weakly, particularly for indoor environments presenting similar collinearity patterns. Ongoing work aims to obtaining a complete registration and mapping pipeline based on the Angular Radon Spectrum formulation.

References

[1] W. Hess, D. Kohler, H. Rapp, and D. Andor, "Real-Time Loop Closure in 2D LIDAR SLAM," in *Proc. of the IEEE Int. Conf. on Robotics & Automation (ICRA)*, 2016, pp. 1271–1278.

[2] H. J. Sohn and B. K. Kim, "Vecslam: an efficient vector-based slam algorithm for indoor environments," *Journal of Intelligent and Robotic Systems*, vol. 56, pp. 301–318, 2009.

[3] M. Himstedt, J. Frost, S. Hellbach, H.-J. Boehme, and E. Maehle, "Large scale place recognition in 2D lidar scans using geometrical landmark relations," in *Proc. of the IEEE/RSJ Int. Conf. on Intelligent Robots and Systems (IROS)*, 2014, pp. 5030–5035.

[4] J. Deray, J. Solà, and J. Andrade-Cetto, "Word ordering and document adjacency for large loop closure detection in 2-d laser maps," *IEEE Robotics and Automation Letters (RA-L)*, vol. 2, no. 3, pp. 1532–1539, 2017.

[5] L. Carlone, A. Censi, and F. Dellaert, "Selecting good measurements via ℓ_1 relaxation: A convex approach for robust estimation over graphs." Georgia Institute of Technology, 2014.

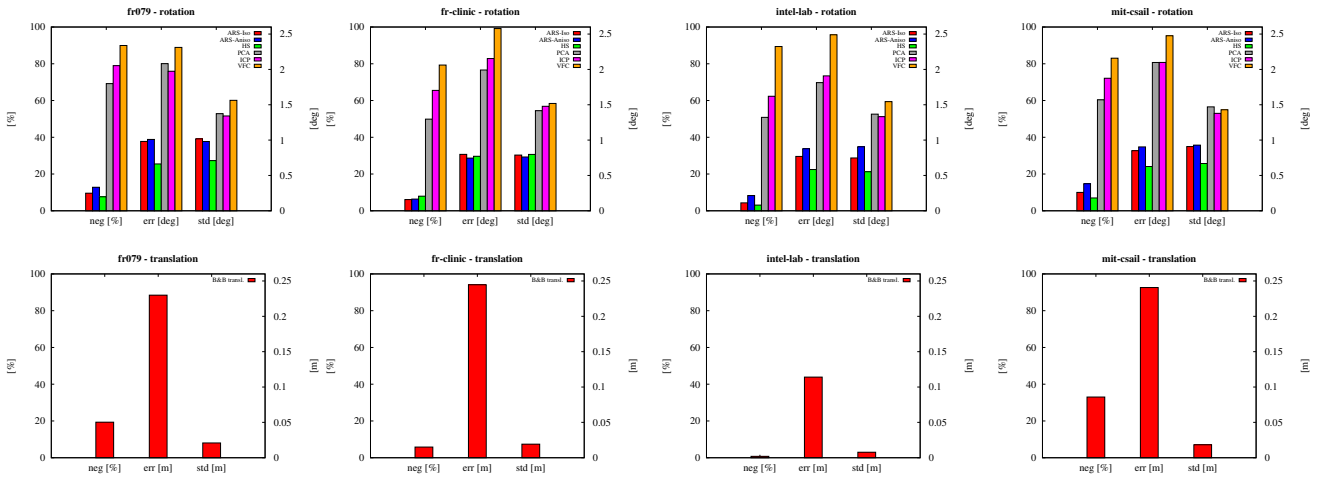

Fig. 2: Registration accuracy in estimation of rotation (top) and of translation (bottom) on scan datasets *fr079*, *fr-clinic*, *intel-lab* and *mit-csail* (from left to right). For each set of tests, negative (failed) estimation percentage, average rotation error [°, respectively $[m]$] are reported.

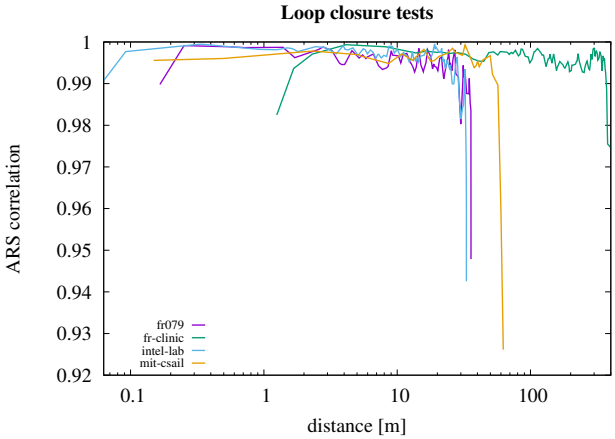

Fig. 3: Correlation between the ARS of two point clouds as a function of their distance in datasets *fr079* (purple), *fr-clinic* (green), *intel-lab* (blue) and *mit-csail* (yellow).

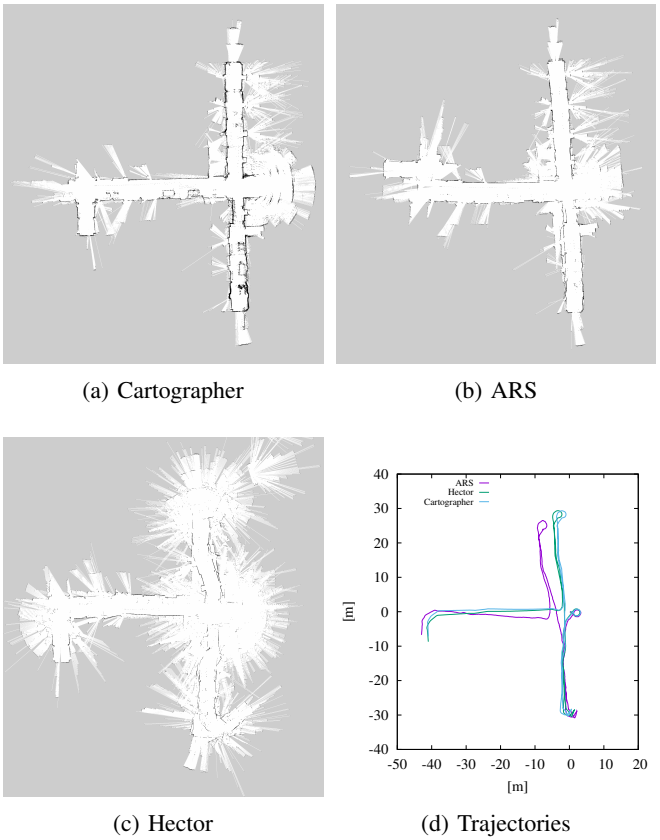

(a) Cartographer (b) ARS

(c) Hector (d) Trajectories

Fig. 4: Occupancy grid maps and estimated trajectories of dataset *uniprdia_1* obtained using Cartographer, Hector SLAM and ARS-based registration. The occupancy grid maps are computed using Octomap that overlaps online raw laser scan data. ARS registration is able to keep track of a non-trivial trajectory with limited error.

[6] H. Yin, X. Xu, S. Lu, X. Chen, R. Xiong, S. Shen, C. Stachniss, and Y. Wang, "A survey on global lidar localization," *arXiv preprint arXiv:2302.07433*, 2023.

[7] D. Lodi Rizzini, "Angular Radon Spectrum for Rotation Estimation," *Pattern Recognition*, vol. 84, pp. 182–196, dec 2018.

[8] D. Lodi Rizzini and E. Fontana, "Rotation Estimation Based on Anisotropic Angular Radon Spectrum," *IEEE Robotics and Automation Letters*, vol. 7, no. 3, pp. 7279–7286, 2022.

[9] S. Deans, "Radon and Abel Transforms," in *The Transforms and Applications Handbook*, 2nd ed., A. Poularikas, Ed. CRC Press, 2000, pp. 1–95.

[10] Y. Liu, C. Wang, Z. Song, and M. Wang, "Efficient global point cloud registration by matching rotation invariant features through translation search," in *Proceedings of the European Conference on Computer Vision (ECCV)*, 2018, pp. 448–463.

[11] S. Kohlbrecher, J. Meyer, O. von Stryk, and U. Klingauf, "A flexible and scalable slam system with full 3d motion estimation," in *Proc. IEEE International Symposium on Safety, Security and Rescue Robotics (SSRR)*. IEEE, November 2011.

[12] A. Hornung, K. Wurm, M. Bennewitz, C. Stachniss, and W. Burgard, "OctoMap: An Efficient Probabilistic 3D Mapping Framework Based on Octrees," *Autonomous Robots*, 2013.